

Article

Industrial Low-Clinker Precast Elements Using Recycled Aggregates

Carlos Thomas ^{1,*}, Ana I. Cimentada ¹, Blas Cantero ², Isabel F. Sáez del Bosque ²
and Juan A. Polanco ¹

¹ LADICIM (Laboratory of Materials Science and Engineering), University of Cantabria E.T.S. de Ingenieros de Caminos, Canales y Puertos, Av. Los Castros 44, 39005 Santander, Spain; anaisabel.cimentada@unican.es (A.I.C.); polancoa@unican.es (J.A.P.)

² School of Civil Engineering, University of Extremadura, Institute for Sustainable Regional Development (INTERRA), Avda. de la Universidad, s/n, 10003 Cáceres, Spain; bcanteroch@unex.es (B.C.); cmedinam@unex.es (I.F.S.d.B.)

* Correspondence: thomasc@unican.es

Received: 31 August 2020; Accepted: 21 September 2020; Published: 23 September 2020



Abstract: Increasing amounts of sustainable concretes are being used as society becomes more aware of the environment. This paper attempts to evaluate the properties of precast concrete elements formed with recycled coarse aggregate and low clinker content cement using recycled additions. To this end, six different mix proportions were characterized: a reference concrete; 2 concretes with 25%wt. and 50%wt. substitution of coarse aggregate made using mixed construction and demolition wastes; and others with recycled cement with low clinker content. The compressive strength, the elastic modulus, and the durability indicator decrease with the proportions of recycled aggregate replacing aggregate, and it is accentuated with the incorporation of recycled cement. However, all the precast elements tested show good performance with slight reduction in the mechanical properties. To confirm the appropriate behaviour of New Jersey precast barriers, a test that simulated the impact of a vehicle was carried out.

Keywords: recycled concrete; low clinker cement; precast; mechanical properties; physical properties; New Jersey barriers

1. Introduction

Construction and demolition waste (CDW) is non-hazardous, inert waste generated in any construction, rehabilitation or demolition work. The industrial and construction sectors generate practically the same amount of non-hazardous waste (industry 37,417 kt[†] and construction 35,869 kt[†]) in Spain [1]. The European Commission estimates that the volume of CDW comprises one third of all waste generated in the European Union, which constitutes the largest waste stream [2]. Recycling this CDW would lead to more sustainable growth, replacing a linear economy based on use of materials with a more circular economy. This is important, as aggregates are the second-most-used raw material by humans, behind only water [3]. There is European legislation to encourage recycling CDW [4] and many countries have specific norms for the use of recycled aggregates (RA) for concrete [5–8]. In addition, the use of RA could lead to cheaper concrete [9].

Several studies have corroborated that the inclusion of RA produces concrete with a lower density and increased heterogeneity [10–12]. RA normally has a higher porosity than natural aggregate (NA) [13]. In a fresh state, Silva et al. [11] concluded that recycled aggregate concrete (RAC) is less workable and, to achieve a workability equivalent to that of NA, RA could be pre-saturated, or water added during mixing to compensate [14]. However, the incorporation of completely saturated

aggregates might cause an excessive water supply [15,16]. Once the RAC hardens, these aggregates make the concrete more susceptible to detrimental environmental effects, resulting in a lower durability [17,18], which should be taken into consideration. Consequently, Annex 15 of the Spanish Instruction for Structural Concrete EHE-08 [19] and other studies [14,20] propose solutions, such as increasing the cement content, reducing the water/cement ratio, or increasing the coating thickness in the case of reinforced concrete.

Generally, it is known that the incorporation of RA into concrete reduces its mechanical properties [21,22], due to the presence of contaminants such as plastics, glass, adhered mortar, etc., ref. [23] and the type of source material (crushed concrete, ceramic or mixed) of the RA [24–26]. The elastic modulus of RAC is lower than that of conventional concrete [15], reaching 45% less for 100% replacement [25]. The results obtained in the characterization of RAC with intermediate replacements present greater variation of results [20]. Other authors have demonstrated the viability of other types of recycled aggregates from waste, such as steel slag [27]. Moreover, the RA affects the fatigue behavior of the concrete [28–32], showing a greater loss of properties than with the static properties. Further research has evaluated the recycling of concrete which incorporates RA [33,34].

With regard to precast concrete elements, it should be noted that, according to the ANDECE (National Association of the Prefabricated Concrete Industry, based in Spain), although the initial cost of elements is higher, the final cost is lower [35]. Other studies such as López-Mesa et al. [36] indicate an almost 18% higher cost of precast slabs versus in situ slabs; although the former have a lower environmental impact and the quality may be higher. Normally, precast elements have a quality seal guaranteeing their properties. Due to a manufacturing process with complete exhaustive control, precast slabs can be: tailored with special properties more easily as they are not manufactured on site; designed with flexibility difficult to achieve in-situ; and incorporate RA in their fabrication. In the case of precast elements using RA, a lower density and strength is observed [37]. Poon et al. [37] investigated the factors that affect the properties of precast concrete blocks with RA, concluding that the compressive strength increases with the reduction in the aggregate/cement ratio (A/C), and that the water absorption of concrete blocks is significantly related to the absorption capacity of the aggregate. Katz [21] investigated the use of precast elements at different ages to produce RA for new precast elements, concluding that the mechanical properties (strength, modulus of elasticity, etc.) when using this type of aggregate in concrete, resemble those when using lightweight aggregates, such as those manufactured using fly ash.

This paper presents the effect on physical and mechanical properties of six types of mixes with different degrees of substitution. The physical properties and durability of these concretes will be analyzed first, then the mechanical properties will be assessed. Finally, the behavior of precast elements will be addressed.

2. Materials and Methodology

The natural siliceous aggregate used in this study is present in three different sizes: 6/0 mm (NS), 12/6 mm (NG-M), and 22/12 mm (NG-C). Mixed recycled aggregates (MRA) were used by substituting NG-M for MRA-M and NG-C for MRA-C. These MRA were obtained from CDW and were principally made up of concrete and mortars ($\approx 45\%$), unbound aggregate, and natural stone ($\approx 45\%$). Figure 1 shows the different size grading for each aggregate.

Table 2. Concrete mix proportions (by m³).

Concrete:	HP	HPR	HR25	HR50	HRR25	HRR50
NS (6/0 mm) [kg]:	732	732	719	705	719	705
NG-M (12/6 mm) [kg]:	382	382	284	184	284	184
NG-C (22/12 mm) [kg]:	766	766	568	369	568	369
MRA-M (12/6 mm) [kg]:	-	-	89	178	89	178
MRA-C (22/12 mm) [kg]:	-	-	178	356	178	356
Cement [kg]:	400	-	400	400	-	-
Low clinker content cement [kg]:	-	400	-	-	400	400
Water [kg]:	193	193	202	211	202	211
Superplasticizer [kg]:	6.2	6.2	6.2	6.2	6.2	6.2
Water/cement ratio	0.48	0.48	0.50	0.53	0.50	0.53

2.1. Physical and Mechanical Properties

Densities were obtained according to EN-12390-7 [41]. Sub-specimens (10Ø × 10 cm) obtained by cutting 10Ø × 20 cm cylindrical specimens were used. The porosity coefficient is the result of comparing the absorbed water and specimen volume, while the absorption coefficient is the result of comparing the absorbed water and specimen weight. Compressive strength was determined using 10Ø × 20 cm cylindrical specimens according to EN-12390-3 [42], with an application strength rate of 0.5 MPa/s. Elastic modulus was determined with 10Ø × 20 cm cylindrical specimens according to EN-12390-13 [43], at a strength rate of 0.5 MPa/s.

2.2. Durability

A water penetration test was performed according to EN-12390-8 [44]. Sub-specimens (10Ø × 10 cm) obtained by cutting 10Ø × 20 cm cylindrical specimens were used. The samples were subjected to a pressure of 5 bar for 72 h. After 72 h water penetration under pressure, it was necessary to analyze how deep the water reached. To be able to observe the interior of the sample, it had to be opened. During this research, the Brazilian method (or indirect tensile strength method) was used to open the sample and analyze its interior. In general, when a cylindrical specimen is subjected to tension along its generatrix, it breaks into two halves, which allows the interior to be analyzed. Once the specimen had been opened, it was possible to measure the penetration depth of the water into the porous concrete. This technique also provided another interesting result: the indirect tensile strength of the concrete. For the determination of oxygen permeability, UNE-83981 [45] was taken as a reference. The 10Ø × 20 cm cylindrical specimens were cut to discard the upper and lower face obtaining a new sample of 10Ø × 10 cm. Silicone was impregnated perimetrically in the samples so that the oxygen could only pass longitudinally. A regulated oxygen pressure was applied on the upper face. Digital flow meters registered the oxygen escaping from the lower face.

2.3. Precast Element Preparation

Two different types of precast elements were manufactured: unreinforced concrete ditches and steel-reinforced New Jersey barriers. Both were manufactured with an industrial concrete mixer, poured in metallic molds and vibrated by hand (Figure 2). In the case of reinforced concrete, reinforcements were set into the mold before the pouring of concrete. In both cases, precast elements were unmolded and cured at ambient temperature.



Figure 2. Precast element manufacturing sequence.

2.4. Precast Element Mechanical Characterization

Concrete ditches have approximate measurements of $50 \times 50 \times 15$ cm. In order to characterize concrete ditches, the tests were carried out by bending. The horizontality of the set was verified, and force was applied by a roller ($10\text{Ø} \times 22$ cm) in the central section with a displacement rate of 0.1 mm/s (Figure 3).

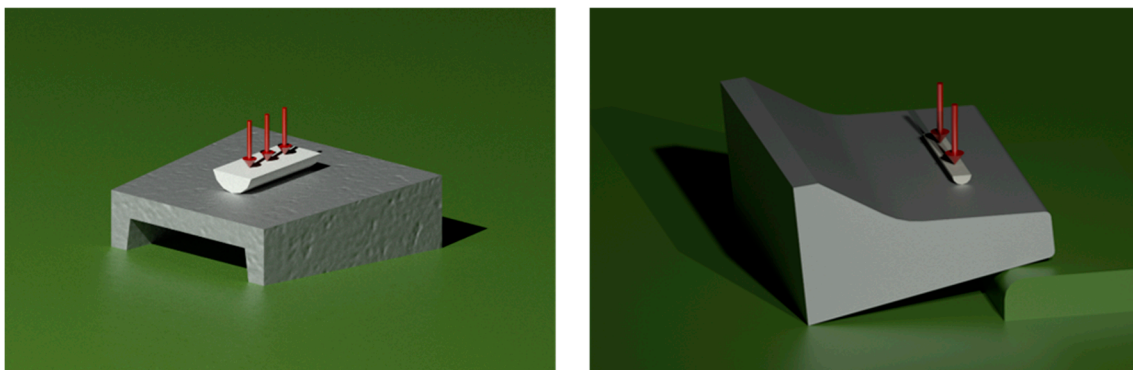


Figure 3. Precast element characterization (concrete ditches left, New Jersey barriers right).

New Jersey barriers have a section with approximate measurements of 47×80 cm and a length of 100 cm. In order to characterize New Jersey barriers, a small crane was used to support the precast element on steel beams. These steel beams were placed at one end to correct the inclination of the face on which the test was to be performed, achieving horizontality on that face (Figure 3). The test consisted in applying a stress with a roller ($3\text{Ø} \times 40$ cm). The time of the test was very short (0.1–0.2 s) to simulate an impact. The strength and displacement data of the actuator were recorded during the test.

3. Results and Discussion

3.1. Physical Properties

Figure 4 shows the relative and saturated densities of the concretes. As demonstrated, the density decreases as the percentage of NA replaced by RA increases. This is due to the lower density of RA. It also becomes clear that the use of this RC does not affect density significantly.

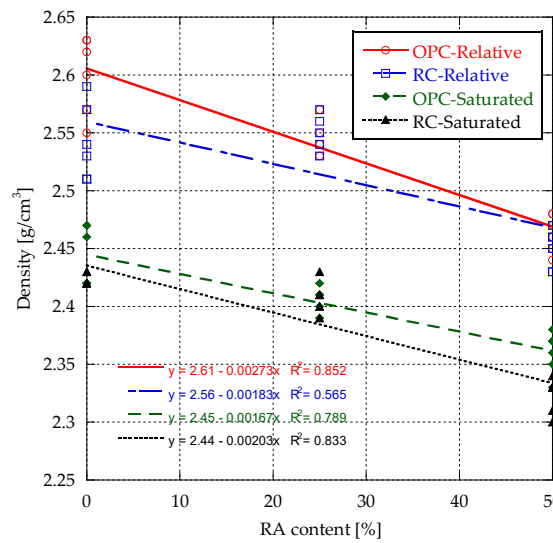


Figure 4. Density vs. RA content.

Figure 5a shows porosity, and Figure 5b shows the absorption coefficient vs. substitution of NA by RA. A decrease in both properties is found in the concretes containing OPC as the percentage of replacement of aggregate increases. However, in the case of concrete made with RC, both properties increase as the percentage of RA increases. This may be because this type of cement interacts more with RAs of different nature, making it difficult to fill all the gaps amongst aggregates. Alternatively, it may be because the RA is able to absorb more water during kneading, causing a small deficit in this type of cement, which is very susceptible to variations in the water dosage. It is possible that there may be another reason that has not been identified.

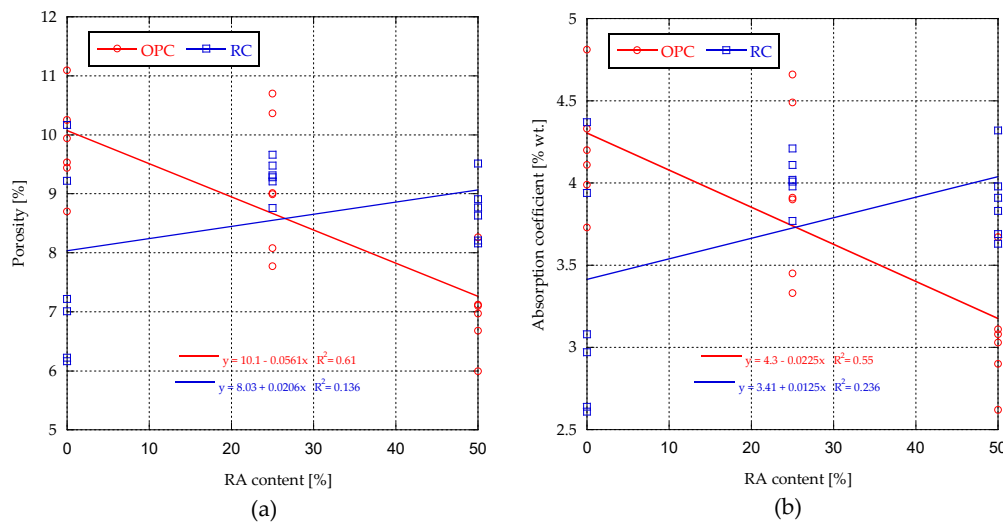


Figure 5. Porosity (a) and absorption coefficient (b) vs. RA content.

3.2. Compressive Strength and Modulus of Elasticity

Figure 6a shows the compressive strength-strain curves for each concrete at 160 days. Several studies [25,46,47] show that the concrete’s compressive strength decreases with the degree of substitution of RA for NA, but in strain terms, concretes show similar values around 2500 $\mu\text{m}/\text{m}$ for the failure. The exception is the HRR50 mix, which exceeds the values of the rest by almost 1000 $\mu\text{m}/\text{m}$. Figure 6b shows the same mixtures but at an age of 365 days. The decrease in strength may also be due to

the randomness of the type of RA and its distribution into the mortar matrix, which causes greater uncertainty than conventional mixtures.

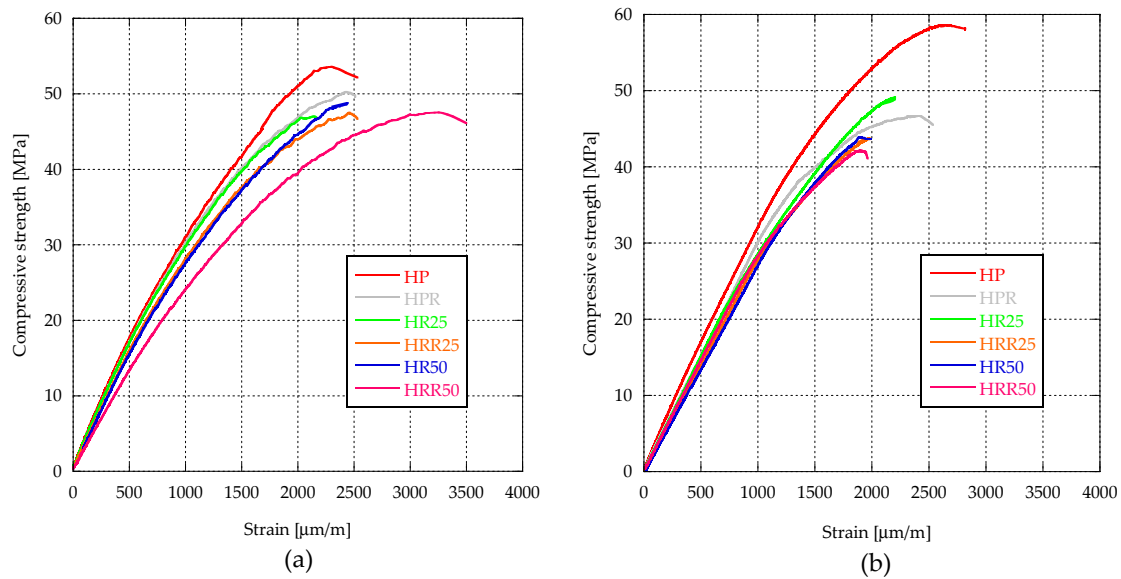


Figure 6. Compressive strength-strain at 160 (a) and 365 (b) days.

Table 3 shows the different values of compressive strength obtained at different ages.

Table 3. Compressive strength at different ages.

Concrete:	Compressive Strength [MPa]			
	28 days	160 days	365 days	Δ_{36-28} [%]
HP	51.2	53.5	56.8	+10.9
HPR	46.1	50.2	46.6	+1.1
HR25	51.7	47.0	45.1	-12.8
HR50	51.2	48.8	42.1	-17.7
HRR25	45.0	47.5	43.7	-2.9
HRR50	41.2	47.5	42.4	+2.9

Table 4 displays the modulus of elasticity, and shows that when using RC, the decrease in the elastic modulus is around 4%. The substitution of 25% by RA implies a decrease in elastic modulus of 5.6%, while the substitution of OPC in this case does not seem to have an influence. In the case of replacing 50% of aggregate by RA, the influence of the substitution of OPC by RC is meaningful, decreasing the elastic modulus by 15%. As for the loss of elastic modulus over time, a greater influence of the cement is observed than the type of aggregate, with a limit that tends to an asymptotic value of around 27 GPa.

Table 4. Modulus of elasticity.

Concrete:	Substitution [%]	Modulus of Elasticity [GPa]	Modulus of Elasticity at 365 days [GPa]	% of the Initial Elastic Modulus
HP	0	35.5	31.7	89.3
HPR	0	34.1	29.5	86.5
HR25	25	33.9	30.8	90.8
HR50	50	31.9	29.3	91.8
HRR25	25	34.2	27.9	81.6
HRR50	50	27.8	27.4	98.6

Some organizations such as EHE-08, ACI, and Eurocode present their expressions to predict elastic modulus at 28 days from the compressive strength. In Expressions (1)–(3): E is elastic modulus at 28 days [GPa] and f_{28} is the compressive strength at 28 days [MPa].

EHE-08 [48]

$$E = 8.5 \sqrt[3]{f_{28}} \tag{1}$$

ACI [49]

$$E = 4.7 \sqrt{f_{28}} \tag{2}$$

Eurocode 2 [50]

$$E = 22(f_{28}/10)^{0.3} \tag{3}$$

These expressions can be used to obtain the predictions and comparisons, with the experimental results shown in Table 5. The ACI method fits quite well in most cases but predicts higher values when the percentage of substitution is 50%. The EHE-08 method is safer, although when the substitution is 50% and the OPC is replaced by RC, higher values are produced due to the heterogeneity of the RA affecting the compressive strength. These types of expressions only satisfactorily fit ordinary concrete models.

Table 5. Elastic modulus obtained with different expressions.

Concrete:	Elastic Modulus [GPa]				
	Experimental	EHE-08	ACI	Eurocode 2	$\Delta_{\text{experimental-EHE-08}}$ [%]
HP	35.5	31.6	33.6	35.9	12.5
HPR	34.1	30.5	31.9	34.8	11.9
HR25	33.9	31.7	33.8	36.0	7.1
HR50	31.9	31.6	33.6	35.9	1.1
HRR25	34.2	30.2	31.5	34.5	13.1
HRR50	27.8	29.4	30.2	33.6	-5.3

Figure 7 shows that from approximately 48 MPa, concrete with RA achieved the same compressive strength as concrete with OPC. RA concrete increases its elastic modulus significantly. This might be due to the addition of a new variable, such as RA compared with OPC, which is much more standardized throughout its production process.

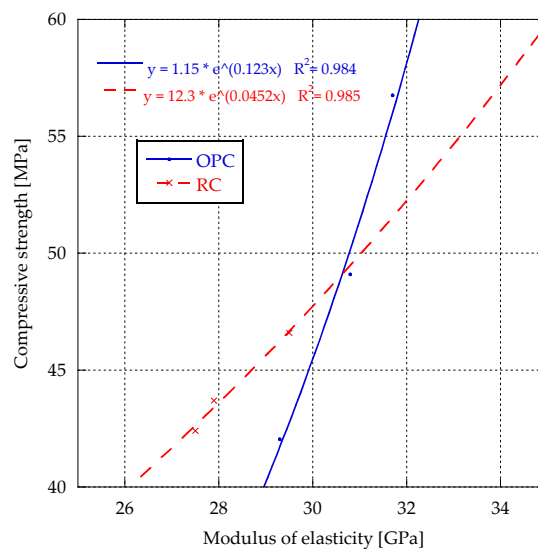


Figure 7. Compressive strength vs. modulus of elasticity.

3.3. Oxygen and Water Permeability

Figure 8a shows the oxygen permeability and Figure 8b shows the maximum penetration of water vs. percentage of substitution, respectively.

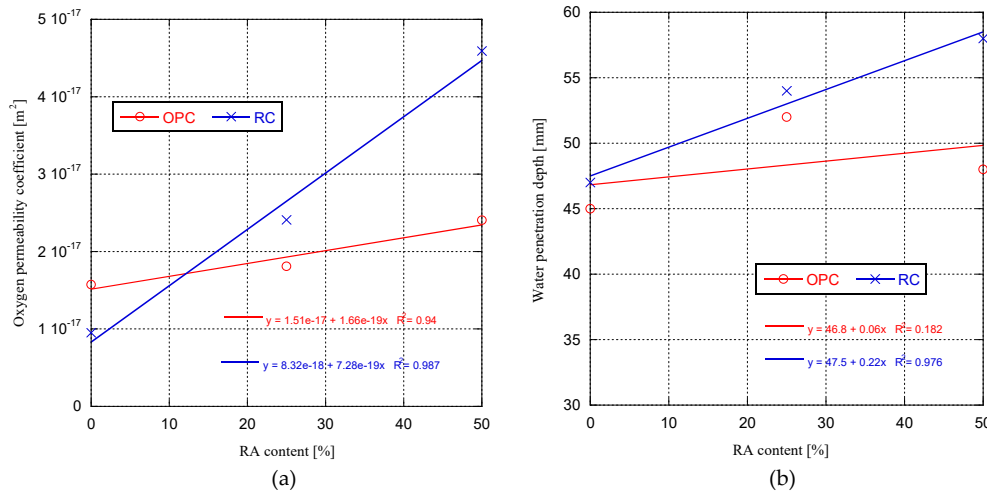


Figure 8. Oxygen permeability coefficient (a) and water penetration depth (b).

The oxygen permeability coefficient increases with the substitution of the NA by RA. This behavior has been reported in some studies, such as Ismail et al. [51], Medina et al. [52], and Thomas et al. [14]. This increase is higher in concrete with RC than OPC; the type of cement being used is an important factor.

The penetration of water increases with the increase in RA substitution. With these results, only HP and HPR comply with the standard EHE-08 [48] for structural concrete in the case of IIIa, IIIb, IV, etc. environment exposition, which requires an average penetration depth of 30mm, and maximum penetration depth of 50 mm. Penetration of water is related to typology and distribution of the RA, and its impurities with high absorption coefficients.

Figure 9 shows cross-sections of concrete where different colors can be seen. These are caused by the RC in HPR and HRR50 mixtures, and some kind of RA and impurities (such as wood or fired clay) in HRR50 mix.

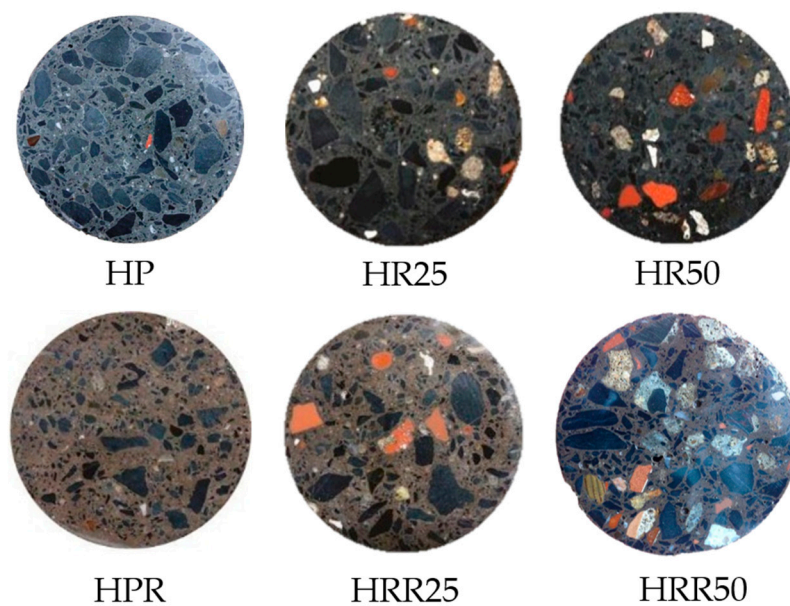


Figure 9. Concrete specimen sections.

3.4. Testing Precast Elements

Figure 10a shows the results of flexural tests on concrete ditches. It can be observed that the concrete composed of RC and RA (HRR50) behaves similarly to HP concrete, which is consistent with the results of splitting tensile strength shown in Table 6. Figure 10b shows the results of the impact test on reinforced precast New Jersey barriers, in which the force applied by the test machine and the position of the actuator are recorded. As expected, the concrete with OPC and NA displayed superior mechanical behavior than concrete with RC and RA. HRR50 could resist only 60% of the force, and 66% of the displacement that HP resisted.

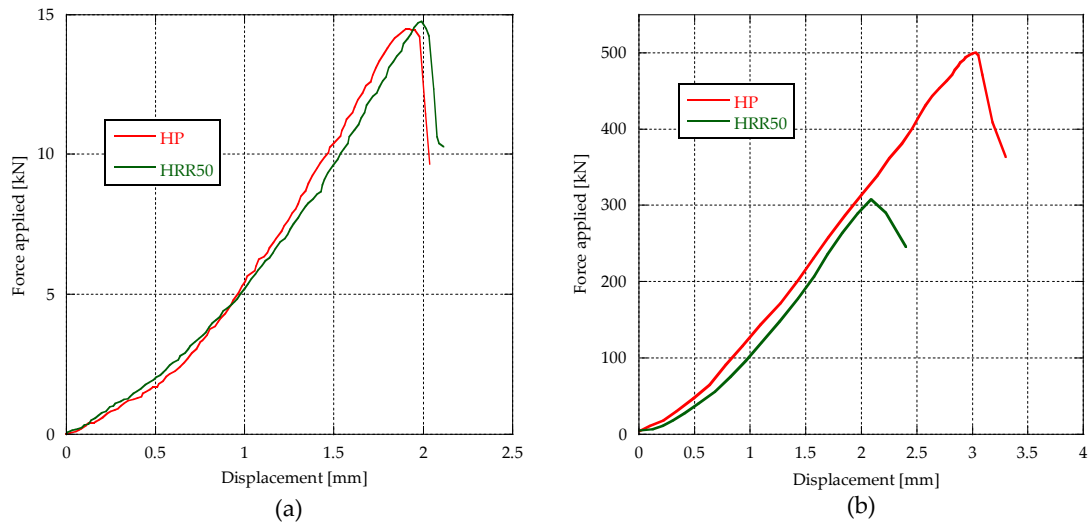


Figure 10. Mechanical characterization of precast elements: Bending test on ditches (a), impact test on barriers (b).

Table 6. Splitting tensile strength.

Splitting Tensile Strength [MPa]					
HP	HPR	HR25	HR50	HRR25	HRR50
3.36	3.51	3.48	-	3.30	3.58

Figure 11 shows the results of the test performed with both types of precast elements. Different sections of cracks in OPC and RC concrete ditches, and the fissure produced in a New Jersey barrier are visual results of the tests.



Figure 11. Precast test and cracking.

Equation (4) indicates whether a New Jersey barrier could withstand the perpendicular impact of a vehicle. Velocity and mass are variables, and it would be necessary to incorporate a restitution coefficient in order to avoid the elastic impact.

This coefficient relates the velocity before impact with the velocity after collision, considering the barrier is without velocity before and after impact.

$$C_R = -\frac{V_{1f} - V_{2f}}{V_{1i} - V_{2i}}; \text{when } V_{2f}, V_{2i} = 0 \rightarrow C_R = -\frac{V_f}{V_i} \tag{4}$$

García and Cabreiro [53] proposed a method for obtaining the coefficient of restitution based on experimental processes in “Use of dynamic models in the investigation of road accidents” (text in Spanish), for which they suggested two equations:

$$C_R = 0.45 \cdot e^{(-0.040278 \cdot v)}, \text{ For } v < 54 \text{ km/h} \tag{5}$$

$$C_R = 0.45 \cdot e^{(-0.015278 \cdot v)}, \text{ For } v \geq 54 \text{ km/h} \tag{6}$$

With Equations (4)–(6), considering the maximum force that a barrier resists, and the duration of the impact as 0.1 s, Equations (7) and (8) are obtained, shown in Figure 12.

$$m = \frac{0.1 \cdot F}{-\left(\frac{v_i}{3.6}\right) \cdot (0.45 \cdot e^{(-0.040278 \cdot v)} + 1)}, \text{ For } v < 54 \text{ km/h} \tag{7}$$

$$m = \frac{0.1 \cdot F}{-\left(\frac{v_i}{3.6}\right) \cdot (0.12 \cdot e^{(-0.015278 \cdot v)} + 1)}, \text{ For } v \geq 54 \text{ km/h} \tag{8}$$

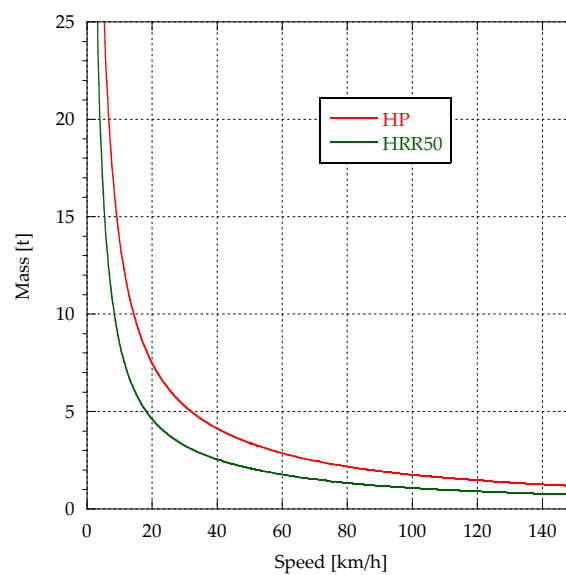


Figure 12. Simulated behavior of reinforced barriers.

These curves are conservative, as the barrier can withstand strains that absorb energy before cracking, and the parapet would not always be immobile (they are only anchored to the ground on viaducts).

4. Conclusions

Characterization tests on concrete specimens and precast elements have been carried out using low-clinker cements and recycled aggregates, obtaining the following conclusions. Firstly, the physical-mechanical properties of mixed recycled aggregates are suitable for the manufacture of

concrete and precast elements when the medium and coarse fraction is used. Secondly, the use of mixed recycled aggregates causes a loss of density and compressive strength slightly higher than that which occurs when using recycled concrete aggregates. Recycled concretes made from low-clinker cement are slightly more porous than concretes made with ordinary Portland cement. Finally, regarding the mechanical properties of recycled concrete, a loss of around 10% of the compressive strength is observed when using low-clinker cement. In addition, recycled concrete made with ordinary Portland cement evolves slightly more when over 1 year of curing has elapsed.

Author Contributions: Conceptualization, C.T., A.I.C., J.A.P.; methodology, C.T., A.I.C., J.A.P., I.F.S.d.B., B.C.; validation, C.T., I.F.S.d.B., B.C.; formal analysis, C.T.; investigation, C.T., A.I.C., J.A.P.; resources, C.T., J.A.P.; writing—original draft preparation, C.T., I.F.S.d.B., B.C.; writing—review and editing C.T. All authors have read and agreed to the published version of the manuscript.

Funding: This research was funded by SODERCAN, S.A. (SODERCAN/FEDER) and BIA2013-48876-C3-2-R awarded by the Ministry of Science and Innovation.

Acknowledgments: The authors would like to express our gratitude to Jaime de la Fuente and César Medina for their support and participation in part of the project.

Conflicts of Interest: Authors declare no conflict of interest.

References

1. Instituto Nacional de Estadística (INE). Estadísticas Sobre Generación de Residuos. Available online: <https://www.ine.es> (accessed on 23 September 2020).
2. UE Comisión Europea. Protocolo de Gestión de Residuos de Construcción y Demolición en la UE. Available online: <https://europa.eu> (accessed on 23 September 2020).
3. ANEFA. Available online: <http://www.aridos.org> (accessed on 23 September 2020).
4. Directiva 2008/98/CE Sobre los Residuos. Available online: <https://eur-lex.europa.eu/eli/dir/2008/98/oj> (accessed on 23 September 2020).
5. Deutsches Institut für Normung. *DIN 4226-100 Aggregates for Concrete and Mortar—Part 100: Recycled Aggregates*; German Institute for Standardisation: Berlin, Germany, 2002.
6. Guobiao Standards. GB/T 25176-2010 Recycled Fine Aggregate from Concrete and Mortar. 2010. Available online: <https://www.gbstandards.org> (accessed on 23 September 2020).
7. Guobiao Standards. GB/T 25177-2010 Recycled Coarse Aggregate for Concrete. 2010. Available online: <https://www.gbstandards.org>. (accessed on 23 September 2020).
8. JIS. *JIS A 5021, Recycled Aggregate for Concrete*; Japanese Standards Association: Tokyo, Japan, 2005.
9. Dimitriou, G.; Savva, P.; Petrou, M.F. Enhancing mechanical and durability properties of recycled aggregate concrete. *Constr. Build. Mater.* **2018**, *158*, 228–235. [[CrossRef](#)]
10. Salesa, Á.; Pérez-Benedicto, J.A.; Colorado-Aranguren, D.; López-Julián, P.L.; Esteban, L.M.; Sanz-Baldúz, L.J.; Sáez-Hostaled, J.L.; Ramis, J.; Olivares, D. Physico-Mechanical properties of multi-Recycled concrete from precast concrete industry. *J. Clean. Prod.* **2017**, *141*, 248–255. [[CrossRef](#)]
11. Silva, R.V.; de Brito, J.; Dhir, R.K. Fresh-state performance of recycled aggregate concrete: A review. *Constr. Build. Mater.* **2018**, *178*, 19–31. [[CrossRef](#)]
12. Centro de Estudios y Experimentación de Obras Públicas (CEDEX). Ministerio de Fomento—Árido Reciclado Cerámico o Mixto. Available online: <http://www.cedex.es/> (accessed on 23 September 2020).
13. Akhtar, A.; Sarmah, A.K. Construction and demolition waste generation and properties of recycled aggregate concrete: A global perspective. *J. Clean. Prod.* **2018**, *186*, 262–281. [[CrossRef](#)]
14. Thomas, C.; Setién, J.; Polanco, J.A.; Alaejos, P.; Sánchez De Juan, M. Durability of recycled aggregate concrete. *Constr. Build. Mater.* **2013**, *40*, 1054–1065. [[CrossRef](#)]
15. Etxeberria, M.; Vázquez, E.; Marí, A.; Barra, M. Influence of amount of recycled coarse aggregates and production process on properties of recycled aggregate concrete. *Cem. Concr. Res.* **2007**, *37*, 735–742. [[CrossRef](#)]
16. Cachim, P.B. Mechanical properties of brick aggregate concrete. *Constr. Build. Mater.* **2009**, *23*, 1292–1297. [[CrossRef](#)]
17. Guo, H.; Shi, C.; Guan, X.; Zhu, J.; Ding, Y.; Ling, T.-C.; Zhang, H.; Wang, Y. Durability of recycled aggregate concrete—A review. *Cem. Concr. Compos.* **2018**, *89*, 251–259. [[CrossRef](#)]

18. Gómez-Soberón, J.M.V. Porosity of recycled concrete with substitution of recycled concrete aggregate: An experimental study. *Cem. Concr. Res.* **2002**, *32*, 1301–1311. [[CrossRef](#)]
19. Ministerio de Fomento. *Gobierno de España EHE-08 ANEJO 15 Recomendaciones para la Utilización de Hormigones Reciclad*os. Available online: <https://www.mitma.gob.es/organos-colegiados/mas-organos-colegiados/comision-permanente-del-hormigon/cph/instrucciones/ehe-08-version-en-castellano> (accessed on 23 September 2020).
20. Rahal, K. Mechanical properties of concrete with recycled coarse aggregate. *Build. Environ.* **2007**, *42*, 407–415. [[CrossRef](#)]
21. Katz, A. Properties of concrete made with recycled aggregate from partially hydrated old concrete. *Cem. Concr. Res.* **2003**, *33*, 703–711. [[CrossRef](#)]
22. Andreu, G.; Miren, E. Experimental analysis of properties of high performance recycled aggregate concrete. *Constr. Build. Mater.* **2014**, *52*, 227–235. [[CrossRef](#)]
23. Silva, R.V.; de Brito, J.; Dhir, R.K. Properties and composition of recycled aggregates from construction and demolition waste suitable for concrete production. *Constr. Build. Mater.* **2014**, *65*, 201–217. [[CrossRef](#)]
24. Hormigón reciclado. *Comisión 2 Grupo de Trabajo 2/5—Utilización de árido Reciclado para la Fabricación de Hormigón Estructural*; ACHE: Madrid, Spain, 2006; ISBN 84-89670-55-2.
25. Xiao, J.; Li, J.; Zhang, C. Mechanical properties of recycled aggregate concrete under uniaxial loading. *Cem. Concr. Res.* **2005**, *35*, 1187–1194. [[CrossRef](#)]
26. Poon, C.S.; Shui, Z.H.; Lam, L. Effect of microstructure of ITZ on compressive strength of concrete prepared with recycled aggregates. *Constr. Build. Mater.* **2004**, *18*, 461–468. [[CrossRef](#)]
27. Sosa, I.; Thomas, C.; Polanco, J.A.; Setién, J.; Tamayo, P. High performance self-compacting concrete with electric arc furnace slag aggregate and cupola slag powder. *Appl. Sci.* **2020**, *10*, 773. [[CrossRef](#)]
28. Sainz-Aja, J.; Carrascal, I.; Polanco, J.A.; Thomas, C. Fatigue failure micromechanisms in recycled aggregate mortar by μ CT analysis. *J. Build. Eng.* **2020**, *28*. [[CrossRef](#)]
29. Sainz-Aja, J.; Thomas, C.; Carrascal, I.; Polanco, J.A.; de Brito, J. Fast fatigue method for self-compacting recycled aggregate concrete characterization. *J. Clean. Prod.* **2020**, *277*, 123263. [[CrossRef](#)]
30. Thomas, C.; Sosa, I.; Setién, J.; Polanco, J.; Cimentada, A.I. Evaluation of the fatigue behavior of recycled aggregate concrete. *J. Clean. Prod.* **2014**, *65*, 397–405. [[CrossRef](#)]
31. Thomas, C.; Setién, J.; Polanco, J.A.; Lombillo, I.; Cimentada, A. Fatigue limit of recycled aggregate concrete. *Constr. Build. Mater.* **2014**, *52*, 146–154. [[CrossRef](#)]
32. Sainz-Aja, J.; Thomas, C.; Polanco, J.A.; Carrascal, I. High-Frequency Fatigue Testing of Recycled Aggregate Concrete. *Appl. Sci.* **2019**, *10*, 10. [[CrossRef](#)]
33. Thomas, C.; de Brito, J.; Cimentada, A.I.A.I.; Sainz-Aja, J.A.J. Macro- and micro- properties of multi-recycled aggregate concrete. *J. Clean. Prod.* **2019**. [[CrossRef](#)]
34. Tamayo, P.; Pacheco, J.; Thomas, C.; de Brito, J.; Rico, J. Mechanical and Durability Properties of Concrete with Coarse Recycled Aggregate Produced with Electric Arc Furnace Slag Concrete. *Appl. Sci.* **2019**, *10*, 216. [[CrossRef](#)]
35. ANDECE. Asociación Nacional de la Industria del Prefabricado de Hormigón. Available online: <https://www.andece.org> (accessed on 1 September 2020).
36. López-Mesa, B.; Pitarch, Á.; Tomás, A.; Gallego, T. Comparison of environmental impacts of building structures with in situ cast floors and with precast concrete floors. *Build. Environ.* **2009**, *44*, 699–712. [[CrossRef](#)]
37. Poon, C.S.; Lam, C.S. The effect of aggregate-to-cement ratio and types of aggregates on the properties of pre-cast concrete blocks. *Cem. Concr. Compos.* **2008**, *30*, 283–289. [[CrossRef](#)]
38. European norm, EN 1097-6—Tests for Mechanical and Physical Properties of Aggregates. Part 6: Determination of Particle Density and Water Absorption. Available online: <https://shop.bsigroup.com/ProductDetail?pid=00000000030218643> (accessed on 1 September 2020).
39. European norm, EN 1097-2—Tests for Mechanical and Physical Properties of Aggregates. Part 2: Methods for the Determination of Resistance to Fragmentation. Available online: <https://shop.bsigroup.com/ProductDetail?pid=00000000030368676> (accessed on 1 September 2020).
40. European norm, EN 933-3—Tests for Geometrical Properties of Aggregates. Part 3: Determination of Particle Shape. Flakiness Index. Available online: <https://shop.bsigroup.com/ProductDetail/?pid=00000000030241876> (accessed on 1 September 2020).

41. European norm, EN 12390-7:2009—Testing Hardened Concrete Part 7: Density of Hardened Concrete. Available online: <https://shop.bsigroup.com/ProductDetail/?pid=000000000030164912> (accessed on 1 September 2020).
42. European norm, EN 12390-3—Testing Hardened Concrete—Part 3: Compressive Strength of Test Specimens. Available online: <https://shop.bsigroup.com/ProductDetail/?pid=000000000030360097> (accessed on 1 September 2020).
43. European norm, EN 12390-13:2013—Testing Hardened Concrete—Part 13: Determination of Secant Modulus of Elasticity in Compression. Available online: <https://shop.bsigroup.com/ProductDetail/?pid=000000000030398745> (accessed on 1 September 2020).
44. European norm, EN 12390-8:2009/1M:2011—Testing Hardened Concrete—Part 8: Depth of Penetration of Water under Pressure. Available online: <https://www.beuth.de/en/standard/une-en-12390-8/123990156> (accessed on 1 September 2020).
45. Spanish norm, UNE 83981—Concrete Durability. Test Methods. Determination to Gas Permeability of Hardened Concrete. Available online: <https://standards.globalspec.com/std/1445618/une-83981> (accessed on 1 September 2020).
46. McGinnis, M.J.; Davis, M.; de la Rosa, A.; Weldon, B.D.; Kurama, Y.C. Strength and stiffness of concrete with recycled concrete aggregates. *Constr. Build. Mater.* **2017**, *154*, 258–269. [[CrossRef](#)]
47. López Gayarre, F.; Suárez González, J.; Blanco Viñuela, R.; López-Colina Pérez, C.; Serrano López, M.A. Use of recycled mixed aggregates in floor blocks manufacturing. *J. Clean. Prod.* **2017**, *167*, 713–722. [[CrossRef](#)]
48. Ministerio de Fomento—Gobierno de España. EHE-08: Code on Structural Concrete. 2008. Available online: http://www.fomento.gob.es/MFOM/LANG_CASTELLANO/ORGANOS_COLEGIADOS/CPH/instrucciones/EHE08INGLES/ (accessed on 23 September 2020).
49. ACI. The American Concrete Institute. Available online: <https://www.concrete.org> (accessed on 23 September 2020).
50. Eurocode 2: Design of concrete structures EN1992-1-1 1992. Available online: https://eurocodes.jrc.ec.europa.eu/doc/WS2008/EN1992_1_Walraven.pdf (accessed on 23 September 2020).
51. Ismail, S.; Kwan, W.H.; Ramli, M. Mechanical strength and durability properties of concrete containing treated recycled concrete aggregates under different curing conditions. *Constr. Build. Mater.* **2017**, *155*, 296–306. [[CrossRef](#)]
52. Medina, C.; Sánchez De Rojas, M.I.; Thomas, C.; Polanco, J.A.; Frías, M. Durability of recycled concrete made with recycled ceramic sanitary ware aggregate. Inter-indicator relationships. *Constr. Build. Mater.* **2016**, *105*, 480–486. [[CrossRef](#)]
53. García, A.; Cabreiro, J.P. Utilización de modelos dinámicos en la investigación de accidentes viales. In Proceedings of the Congreso Iberoamericano De Accidentología Vial, Avellaneda, Argentina, 9–11 October 2003.



© 2020 by the authors. Licensee MDPI, Basel, Switzerland. This article is an open access article distributed under the terms and conditions of the Creative Commons Attribution (CC BY) license (<http://creativecommons.org/licenses/by/4.0/>).